

Probing Randall-Sundram Model using triphotons at the LHC

David Atwood¹ and Sudhir Kumar Gupta²

*Department of Physics & Astronomy
Iowa State University, Ames, IA 50010 USA*

Abstract

We investigate triphoton signals of the Randall-Sundram model at the Large Hadron Collider. Such a signal can be an important probe to the RS model as these are relatively cleaner from the hadronic activity and bear significant rate. The corresponding standard model background has also been studied in detail. We also show that a clear graviton reconstruction is possible in such signal.

¹E-mail address: atwood@iastate.edu

²E-mail address: skgupta@iastate.edu

1 Introduction

Phenomenology of models based on extra spatial dimensions [1] is quite popular now. Besides offering a solution to the hierarchy problem of the Standard Model [2] these models allow for the low-energy unification of the gauge couplings [3], provide a rich TeV scale new physics phenomenology, existence of gravity at the TeV scale and may even offer candidate(s) for the cold dark matter of the universe [4].

In the simplest string theory inspired extension of the standard model (SM) based on one extra spatial dimension, originally proposed by Randall-Sundrum (RS) [5, 6], gravitons are the only propagating particles in the bulk. Such gravitons will therefore have Kaluza-Klein (KK) excitations which will appear in experiments as a widely separated resonances. This contrasts with the KK spectrum of models with compact extra dimensions such as ADD [7] where there are a very large number of closely spaced graviton modes.

The coupling of these graviton excitations to the SM is through the 4-d reduced Planck mass \bar{M}_P , which may be on the TeV scale, rather than the inaccessibly large Planck mass at 10^{19} GeV. The couplings to Standard Model particles are therefore be proportional to $\sim 1/\bar{M}_P$, thereby allowing graviton excitations to decay into all the SM particles including a fermion pair or a pair of gauge bosons. At TeV scale energies, when such graviton excitations are produced, this variety of possible decay modes will give rise to vast phenomenology at the TeV scale; $\Lambda = \bar{M}_P e^{-\kappa r_c \pi}$, with $e^{-\kappa r_c \pi}$ as a warped factor which arise due to the compactification of the extra dimension on a circle with radius r_c . The factor π is due to the fact that SM is located on the circle at $\phi = \pi$ and κ is the curvature parameter.

Although lots of variations of the RS model have been proposed over the years [8] and their phenomenology [9] has been studied in detail, in this paper we will consider the original scenario. In particular, we assume that the whole the SM is localized on the TeV brane, so that the mass of gravitons is given by $m_{G_n} = x_n \kappa e^{-\kappa r_c \pi} = x_n (\kappa/\bar{M}_P) \Lambda$, where x_n are the roots of the first-order Bessel function. In order to be useful in the resolution of the hierarchy problem and keep gravity weak enough to be treated perturbatively, κ/\bar{M}_P should lie in the range $0.001 < \kappa/\bar{M}_P < 0.1$.

The focus of this paper will be the distinctive triphoton signature at the Large Hadron Collider (LHC) produced by the RS model and other models like it. The importance of such a signature lies in the fact that this signature is experimentally clean and a distinctive signature for models of this type. We will also discuss graviton mass reconstruction and the angular distribution of the graviton decay which are important tools for characterizing the physics which produces the triphoton signal.

The paper is organized as follow: In section 2, we discuss the graviton production in association with a photon and its decays into the SM particles. Section 3 focuses on the numerical analysis of signal and background as well as graviton reconstruction in detail. Finally, in section 4, we summarize our findings.

2 Graviton Production and Decay

Triphoton signal in the RS model will arise due to the associated production of a on shell graviton with a photon while the graviton subsequently decays into an additional photon pair. In this section we discuss the production process as well as the various other dominant two body decays of the graviton.

The parton-level matrix-element for the production process $q\bar{q} \rightarrow \gamma G$ as calculated in [10] is,

$$|\mathcal{M}|^2 = N_c Q_f^2 \left(\frac{3\pi\alpha}{2} \right) \left(\frac{\hat{s}}{M_P^2} \right) F(\eta, \zeta), \quad (1)$$

$$F(\zeta, \eta) = f(\zeta) + f(\eta) + \zeta\eta \left(\frac{1}{\zeta}\phi(\zeta) + \frac{1}{\eta}\phi(\eta) \right) \quad (2)$$

with,

$$\begin{aligned} f(\zeta) &= 1 - \zeta^2 + \zeta^3, \\ \phi(\zeta) &= \zeta(2 - 11\zeta + 4\zeta^2), \end{aligned}$$

where, $\zeta = \frac{\hat{t}}{\hat{s}}$ and $\eta = \frac{\hat{u}}{\hat{s}}$. N_c is the number of colors, $N_c = 3$ and Q_f is the quark charge, $Q_f = +2/3, 1/3$ for up and down type quarks respectively.

The kinematics of this process implies that $m_G^2 = \hat{s}^2 + \hat{t}^2 + \hat{u}^2$. Note that this cross-section is symmetric with respect to the interchange of \hat{t} and \hat{u} .

The LHC production cross-section for this process is presented in Figure 1. We use a wide range of graviton mass well above the Tevatron bounds [11] for three different sets of center-of-mass energy, \sqrt{s} as 7 TeV, 10 TeV, and, 14 TeV respectively. We use CTEQ6L-1[12] parton densities at $Q = \sqrt{\hat{s}}$, and the renormalization and factorization scales are set as, $\mu_R = Q = \mu_F$.

From the Figure 1, it is quite clear that due to the low cross-section, it is hard to observe such productions with the early LHC data with an integrated luminosity of 100 pb⁻¹ and $\sqrt{s} = 10$ TeV. For instance only 2 events would be produced if $m_G = 1$ TeV; at the higher energy $\sqrt{s} = 14$ TeV, the number of events is roughly doubled.

In Figure 2, we present the branching fractions of graviton to various two-body SM mode. The dominant mode is the dijet channel with a branching ratio $B(\rightarrow gg, q_i\bar{q}_i) \sim 64\%$ (where, $i = u, d, s, c, b$). The fraction for the diphoton mode is smaller, $\sim 4\%$, but it is important as this will lead to a clean signature at the LHC.

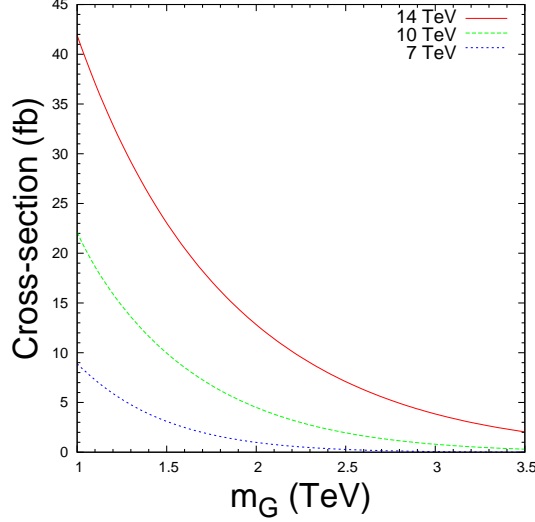


Figure 1: Cross-section for associated production of a Graviton with a photon at the LHC for center-of-mass energy $\sqrt{s} = 7$ TeV, 10 TeV and 14 TeV.

3 Triphotons at the LHC

The production of a graviton associated with a photon occurs in the high x -region, so generally the associated photon as well as the photons produced in the graviton decay will carry high transverse momentum. Large transverse momentum cuts on the triphoton signal will therefore be helpful in selecting graviton events and rejecting SM backgrounds where photons tend to have low transverse momentum.

we use **MADGRAPH** [13, 14] to produce signal events with a photon and a graviton. Later, these events are interfaced to **PYTHIA** [15] for the analysis purpose. Decay of graviton is done using the decay table in **PYTHIA**. Branching fractions for different decay modes for $m_G = 1$ TeV are shown in Fig. 2.

Before selecting our event samples, we order the photons on the basis of their transverse momentum i.e., $p_{T_{\gamma_1}} > p_{T_{\gamma_2}} > p_{T_{\gamma_3}}$.

In order to analyze the actual event rate expected to observe at the LHC, we first employ the following three basic cuts:

- $p_{T_{\gamma_{1,2,3}}} > 25$ GeV and $|\eta_{\gamma_{1,2,3}}| < 2.7$,
- Photon-photon separation, $\Delta R_{\gamma_i \gamma_j} = \sqrt{(\eta_i - \eta_j)^2 + (\phi_i - \phi_j)^2} > 0.2$; $i, j = 1, 2, 3$, $i \neq j$, η_i being psuedo-rapidity of photon i and is defined as $\eta_i = -\ln(\tan \theta_i/2)$.
- Missing transverse energy, $\cancel{E}_T < 30$ GeV.

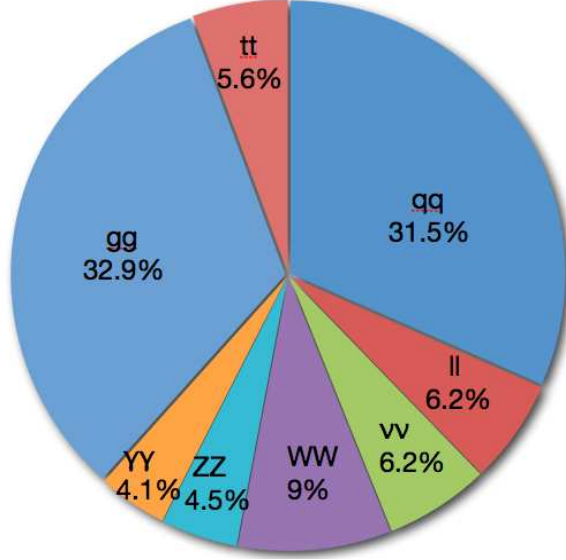


Figure 2: Branching fractions for Graviton decays into standard model particles. $m_G = 1$ TeV has been assumed in this chart.

3.1 SM Background

The SM background is mostly composed of (a) the direct triphoton production i.e. where three photons are produced by SM processes, and (b) processes involving fake photons, in other words, where the detector incorrectly identifies particles which are not photons as photons.

In order to estimate the SM background we use MADGRAPH with the same parton densities as for the signal case. At 14 TeV, the total cross-section for the direct triphoton production in the SM is 0.11 pb. The most likely fake photon backgrounds are those due to the misidentification of jet or an electron as a photon. We can thus subdivide the processes in case (b) as follows:

- (i) Jet induced: jjj , $jj\gamma$, $j\gamma\gamma$, and,
- (ii) Electron induced: $\gamma\gamma e^\pm$, γe^+e^- and $e^\pm e^+e^-$.
- (iii) Both jet and electron induced: je^+e^- , jje^\pm , $j\gamma e^\pm$.

We found that the bare cross-sections for these processes are $\sigma(jjj) = 3.1 \times 10^7$ pb, $\sigma(jj\gamma) = 4.4 \times 10^4$ pb and, $\sigma(j\gamma\gamma) = 99.7$ pb. With the fake probability for a jet to be identified as a photon, $f_{j \rightarrow \gamma} = 1.1 \times 10^{-3}$, as given in [16], the contributions due to these channels to the triphoton background will be 0.04 pb, 0.05 pb and 0.11 pb respectively.

Cross-sections for the processes involving electrons (and positrons) are $\sigma(e^\pm\gamma\gamma) = 0.05$ pb, $\sigma(e^+e^-\gamma) = 10.1$ pb, and, $\sigma(e^\pm e^+e^-) = 0.05$ pb. By assuming a fake rate similar to that

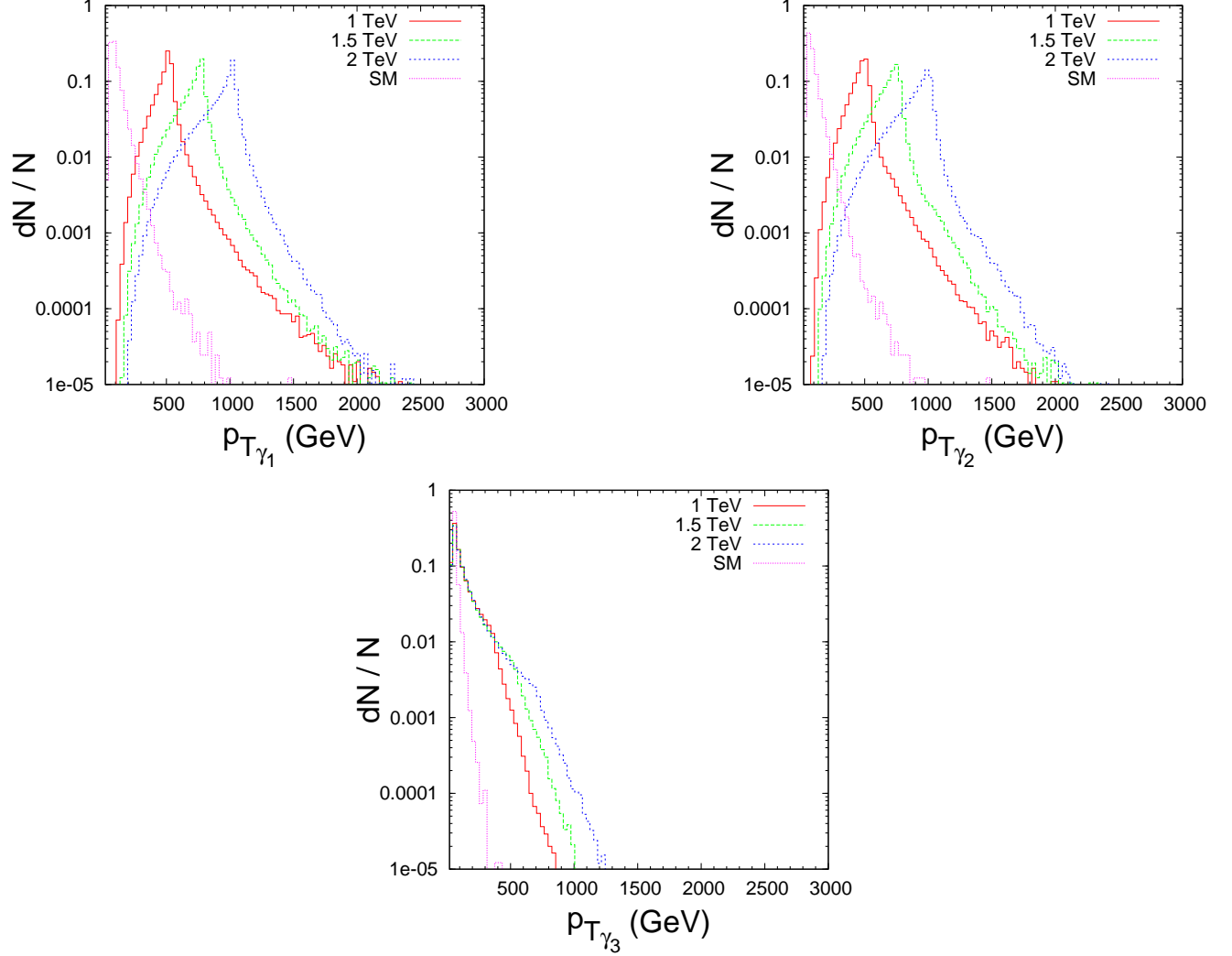


Figure 3: p_T ordered distributions of the photons. We assume $P_{T_{\gamma_1}} > P_{T_{\gamma_2}} > P_{T_{\gamma_3}}$ in this figure.

of a jet the net contribution to the background from these processes will be 6.2×10^{-5} pb which is mostly due to the process involving one electron or a positron arising due to a W production, where W decays into an electron or a positron and the corresponding neutrino or anti-neutrino.

Contribution due to processes involving one or more jets and electrons (or positrons) is 2.5×10^{-5} pb which is also insignificant even though the bare rates are 290.1 pb, 535.3 pb and 19.9 pb for je^+e^- , jje^\pm , $j\gamma e^\pm$ respectively.

The background from fake photons due to jets is the highest with a combined cross-section of $\simeq .2$ pb which is about two times larger than the direct SM triphoton background.

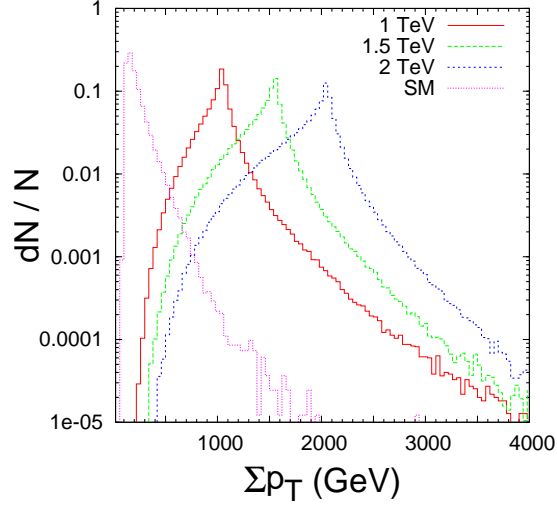


Figure 4: Scalar p_T distributions for the signal and the background. Choices of colors are the same as in Figure 3.

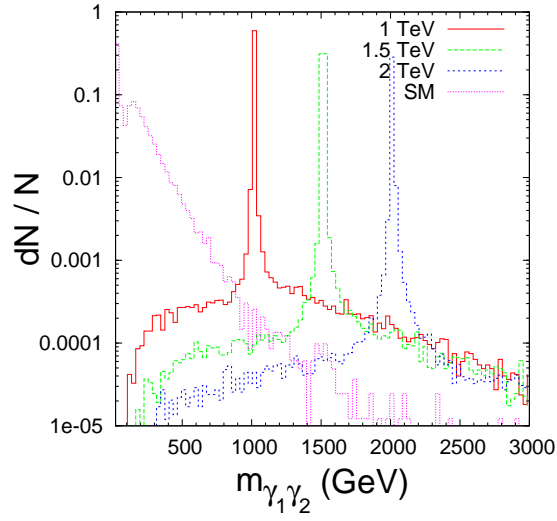


Figure 5: Reconstructed graviton mass from the correct diphoton pair. Choices of colors are the same as in Figure 3

3.2 Results and Graviton Reconstruction

In Figures 3, 4 and 5, we present p_T , Σp_T and invariant mass m_{12} distributions with basic cuts for three different values of graviton mass in case of signal, and, the net background due to direct tri-photons and faked backgrounds due to electrons (or positrons) and photons as discussed above. From Figures 3, it is clear that a demand of $p_{T_{\gamma_{1,2}}} > 100$ GeV and $p_{T_{\gamma_3}} > 50$ GeV will ensure that the triphotons are indeed due to the a heavy graviton production. We employ further cuts on the scalar sum of photons transverse momenta, Σp_T and invariant mass of harder photons, m_{12} . Effects of these individual and combined cuts on the signal and background event rates for an LHC luminosity $\int \mathcal{L} dt = 300 \text{ fb}^{-1}$ is presented in Table 1. As it clear from the Table 1 that, though a large fraction of the background is already eliminated at the basic level itself due to the demand that the missing transverse energy per event should not exceed 30 GeV limit. Yet a cut on scalar sum of the transverse momenta of all the photons, Σp_T of about 550 GeV or alternatively, m_{12} of about 800 GeV in addition to the basic and photon selection cuts reduces the background significantly. A combination of all these cuts reduces to background events to 14 while keeping signals events to 293, 213 and 105 respectively for the graviton mass 1, 1.5 and 2 TeV respectively for an integrated luminosity of 300 fb^{-1} .

In order to reconstruct the graviton mass we use the following techniques: We first reconstruct all possible diphoton pairs with the p_T ordered photons. Later we drop those pairs in each event which are nearer to each other, i.e., those with $|\Delta m_{ij}| < 20$ GeV where, $\Delta m_{ij} = m_{ij}^a - m_{ij}^b$ is the difference of reconstructed invariant masses. Clearly with this technique we are able to help a graviton mass with an uncertainty within 5 – 10 per cent even in the presence of background as shown in Figure 5.

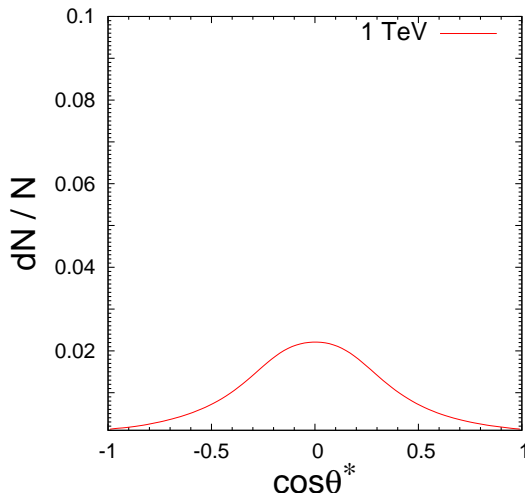


Figure 6: Angular distribution of the decayed photon in the graviton rest frame. $m_G = 1 \text{ TeV}$ is assumed here.

Cuts	SP1	SP2	SP3	SM Background
Basic	454	336	173	8516
$p_{T_{\gamma_{1,2}}} > 100 \text{ GeV}, p_{T_{\gamma_3}} > 50 \text{ GeV}, \Sigma p_T > 550 \text{ GeV}$	454	335	170	142
$p_{T_{\gamma_{1,2}}} > 100 \text{ GeV}, p_{T_{\gamma_3}} > 50 \text{ GeV}, m_{\gamma_1\gamma_2} > 800 \text{ GeV}$	293	214	108	40
Combined	293	213	105	14

Table 1: Efficiency of cuts on signal and background triphoton events for an integrated LHC luminosity of 300 fb^{-1}

Once we have reconstructed the graviton mass, the next task is to measure its spin in order to ensure that the photons are indeed due to decay of a RS graviton. In order to do so, we first identify the correct photon pair which yield the right graviton mass peak in a clean signature case. Next, we boost the photon pair into the rest frame of the graviton. In this boosted frame we produce angular distribution of either of the photons as the two have nearly identical shape. We plot angular distribution for the first photon in Figure 6.

4 Summary and Conclusion

We have studied triphoton signals in details. With a detailed study on background arising due to various SM processes including the processes where a photon can be faked by a jet or an electron or positron. We found that the processes is relatively clean and the background may be greatly reduced (see the Table 1). We have also shown that the graviton mass reconstruction and its spin measurement is possible in this signals though we need to wait for 300 fb^{-1} data in order to have sufficient statistics at the LHC.

Acknowledgments

SKG thanks C Chen and J Cochran for valuable discussions on the SM background. This work was supported in part by a DOE grant under contract number DE-FG02-01ER41155.

References

- [1] See for example, R. Rattazzi, *Proc. of Cargese School of Particle Physics and Cosmology*, Corsica, France, 4-16 Aug 2003; J. Hewett and M. Spiropulu, *Ann. Rev. Nucl. and Part. Sci.* **52**, 397 (2002); C. Csaki, arXiv:hep-ph/0404096; R. Sundrum, arXiv:hep-th/0508134.
- [2] S. Weinberg, *Phys. Rev. D* **13**, 974 (1976), E. Gildener, *Phys. Rev. D* **14**, 1667 (1976); *Phys. Rev. D* **19**, 1277 (1979); L. Susskind, *Phys. Rev. D* **20**, 2619 (1979); G. 't Hooft,

in *Recent developments in gauge theories*, Proceedings of the NATO Advanced Summer Institute, Cargese 1979, (Plenum, 1980).

- [3] L. Randall and M. D. Schwartz, JHEP **0111**, 003 (2001) [arXiv:hep-th/0108114]; L. Randall and M. D. Schwartz, Phys. Rev. Lett. **88**, 081801 (2002) [arXiv:hep-th/0108115]; W. D. Goldberger and I. Z. Rothstein, Phys. Rev. D **68**, 125011 (2003) [arXiv:hep-th/0208060]; K. w. Choi and I. W. Kim, Phys. Rev. D **67**, 045005 (2003) [arXiv:hep-th/0208071]; K. Agashe, A. Delgado and R. Sundrum, Annals Phys. **304**, 145 (2003) [arXiv:hep-ph/0212028].
- [4] K. Agashe and G. Servant, Phys. Rev. Lett. **93**, 231805 (2004) [arXiv:hep-ph/0403143]; K. Agashe and G. Servant, JCAP **0502**, 002 (2005) [arXiv:hep-ph/0411254]; A. Pomarol, Phys. Rev. Lett. **85**, 4004 (2000) [arXiv:hep-ph/0005293].
- [5] L. Randall and R. Sundrum, Phys. Rev. Lett. **83**, 4690 (1999) [arXiv:hep-th/9906064].
- [6] L. Randall and R. Sundrum, Phys. Rev. Lett. **83**, 3370 (1999) [arXiv:hep-ph/9905221].
- [7] N. Arkani-Hamed, S. Dimopoulos and G. R. Dvali, Phys. Lett. B **429**, 263 (1998) [arXiv:hep-ph/9803315]; I. Antoniadis, N. Arkani-Hamed, S. Dimopoulos and G. R. Dvali, Phys. Lett. B **436**, 257 (1998) [arXiv:hep-ph/9804398]; N. Arkani-Hamed, S. Dimopoulos and G. R. Dvali, Phys. Rev. D **59**, 086004 (1999) [arXiv:hep-ph/9807344].
- [8] N. Arkani-Hamed, S. Dimopoulos, G. R. Dvali and N. Kaloper, Phys. Rev. Lett. **84**, 586 (2000) [arXiv:hep-th/9907209]; J. D. Lykken and L. Randall, JHEP **0006**, 014 (2000) [arXiv:hep-th/9908076]; I. Oda, Phys. Lett. B **480**, 305 (2000) [arXiv:hep-th/9908104]; C. Csaki and Y. Shirman, Phys. Rev. D **61**, 024008 (2000) [arXiv:hep-th/9908186]; I. Oda, Phys. Lett. B **472**, 59 (2000) [arXiv:hep-th/9909048]; T. j. Li, arXiv:hep-th/9911234; H. Davoudiasl, J. L. Hewett and T. G. Rizzo, Phys. Rev. Lett. **84**, 2080 (2000) [arXiv:hep-ph/9909255]; I. I. Kogan, S. Mouslopoulos, A. Papazoglou, G. G. Ross and J. Santiago, Nucl. Phys. B **584**, 313 (2000) [arXiv:hep-ph/9912552].
- [9] H. Davoudiasl, J. L. Hewett and T. G. Rizzo, Phys. Lett. B **473**, 43 (2000) [arXiv:hep-ph/9911262]; *ibid.* Phys. Rev. Lett. **84**, 2080 (2000) [arXiv:hep-ph/9909255]. A. Pomarol, Phys. Lett. B **486**, 153 (2000) [arXiv:hep-ph/9911294]; Y. Grossman and M. Neubert, Phys. Lett. B **474**, 361 (2000) [arXiv:hep-ph/9912408]; K. Agashe, A. Delgado, M. J. May and R. Sundrum, JHEP **0308**, 050 (2003) [arXiv:hep-ph/0308036].
- [10] S. Raychaudhuri and S. K. Gupta, in preparation.
- [11] V. M. Abazov *et al.* [D0 Collaboration], Phys. Rev. Lett. **100**, 091802 (2008) [arXiv:0710.3338 [hep-ex]].
- [12] H. L. Lai *et al.*, Phys. Rev. D **51**, 4763 (1995) [arXiv:hep-ph/9410404].
- [13] F. Maltoni and T. Stelzer, JHEP **0302**, 027 (2003) [arXiv:hep-ph/0208156].

- [14] K. Hagiwara, J. Kanzaki, Q. Li and K. Mawatari, Eur. Phys. J. C **56**, 435 (2008) [arXiv:0805.2554 [hep-ph]].
- [15] T. Sjostrand, S. Mrenna and P. Skands, JHEP **0605**, 026 (2006) [arXiv:hep-ph/0603175].
- [16] G. Aad *et al.* [The ATLAS Collaboration], arXiv:0901.0512 [hep-ex].